

---

---

## CHAPTER 4

# Isothermal Titration Calorimetry: Experimental Design, Data Analysis, and Probing Macromolecule/Ligand Binding and Kinetic Interactions

**Matthew W. Freyer and Edwin A. Lewis**

Department of Chemistry and Biochemistry  
Northern Arizona University  
Flagstaff, Arizona 86011

---

Abstract

- I. Introduction
- II. Calorimetry Theory and Operation
  - A. Heat Change Measurement and Theory
  - B. Variations in Ligand/Macromolecule Mixing Techniques
  - C. Commercial Availability
- III. Thermodynamic ITC Experiments
  - A. Preface and Review of Basic Thermodynamics
  - B. Planning the Thermodynamic ITC Experiment
  - C. Running the Thermodynamic ITC Experiment
  - D. Analyzing Thermodynamic Data
  - E. Models
  - F. Error Analysis/Monte Carlo
  - G. Summary
- IV. Kinetic ITC Experiments
  - A. Reaction Rate Versus Heat Rate
  - B. Planning the Experiment
  - C. Running the Kinetic ITC Experiment
  - D. Analyzing the Kinetic ITC Data
  - E. Models
  - F. Summary
- V. Conclusions
- References

---

---

---

## Abstract

Isothermal titration calorimetry (ITC) is now routinely used to directly characterize the thermodynamics of biopolymer binding interactions and the kinetics of enzyme-catalyzed reactions. This is the result of improvements in ITC instrumentation and data analysis software. Modern ITC instruments make it possible to measure heat effects as small as  $0.1 \mu\text{cal}$  ( $0.4 \mu\text{J}$ ), allowing the determination of binding constants,  $K$ 's, as large as  $10^8$ – $10^9 \text{ M}^{-1}$ . Modern ITC instruments make it possible to measure heat rates as small as  $0.1 \mu\text{cal/sec}$ , allowing for the precise determination of reaction rates in the range of  $10^{-12} \text{ mol/sec}$ . Values for  $K_m$  and  $k_{\text{cat}}$ , in the ranges of  $10^{-2}$ – $10^3 \mu\text{M}$  and  $0.05$ – $500 \text{ sec}^{-1}$ , respectively, can be determined by ITC. This chapter reviews the planning of an optimal ITC experiment for either a binding or kinetic study, guides the reader through simulated sample experiments, and reviews analysis of the data and the interpretation of the results.

---

---

---

## I. Introduction

In biology, particularly in studies relating the structure of biopolymers to their functions, two of the most important questions are (i) how tightly does a small molecule bind to a specific interaction site and (ii) if the small molecule is a substrate and is converted to a product, how fast does the reaction take place?

Perhaps the first question we need to ask here is why calorimetry? The calorimeter, in this case an isothermal titration calorimeter (ITC), can be considered a universal detector. Almost any chemical reaction or physical change is accompanied by a change in heat or enthalpy. A measure of the heat taken up from the surroundings (for an endothermic process) or heat given up to the surroundings (for an exothermic process) is simply equal to the amount of the reaction that has occurred,  $n$  (in moles, mmoles,  $\mu\text{moles}$ , nmoles, etc.) and the enthalpy change for the reaction,  $\Delta H$  (typically in kcal/mol or kJ/mol). A measure of the rate at which heat is exchanged with the surroundings is simply equal to the rate of the reaction,  $\partial n/\partial t$  (in moles/sec, mmoles/sec,  $\mu\text{moles/sec}$ , nmoles/sec) and again the enthalpy change,  $\Delta H$ . A calorimeter is therefore an ideal instrument to measure either how much of a reaction has taken place or the rate at which a reaction is occurring. In contrast to optical methods, calorimetric measurements can be done with reactants that are spectroscopically silent (a chromophore or fluorophore tag is not required), can be done on opaque, turbid, or heterogeneous solutions (e.g., cell suspensions), and can be done over a range of biologically relevant conditions (temperature, salt pH, etc.). Although not a topic covered in this chapter, calorimetric measurements have been used to follow the metabolism of cells or tissues in culture over long periods of time and under varying conditions (e.g., anaerobic or aerobic) (Bandman *et al.*, 1975; Monti *et al.*, 1986).

Titration calorimetry was first described as a method for the simultaneous determination of  $K_{\text{eq}}$  and  $\Delta H$  about 40 years ago by Christensen and Izatt (Christensen *et al.*, 1966; Hansen *et al.*, 1965). The method was originally applied to a variety of weak acid–base equilibria and to metal ion complexation reactions (Christensen *et al.*, 1965, 1968; Eatough, 1970). These systems could be studied with the calorimetric instrumentation available at the time which was limited to the determination of equilibrium constant,  $K_{\text{eq}}$ , values less than about  $10^4$ – $10^5 \text{ M}^{-1}$  (Eatough *et al.*, 1985). The determination of larger association constants requires more dilute solutions and the calorimeters of that day were simply not sensitive enough.

Beaudette and Langerman published one of the first calorimetric binding studies of a biological system using a small volume isoperibol titration calorimeter (Beaudette and Langerman, 1978). In 1979, Langerman and Biltonen published a description of microcalorimeters for biological chemistry, including a discussion of available instrumentation, applications, experimental design, and data analysis and interpretation (Biltonen and Langerman, 1979; Langerman and Biltonen, 1979). This was really the beginning of the use of titration calorimetry to study biological equilibria. It took another 10 years before the first commercially available titration calorimeter specifically designed for the study of biological systems became available from MicroCal (Wiseman *et al.*, 1989). This first commercial ITC was marketed as a device for “Determining  $K$  in Minutes” (Wiseman *et al.*, 1989).

ITC is now routinely used to directly characterize the thermodynamics of biopolymer binding interactions (Freire *et al.*, 1990). This is the result of improvements in ITC instrumentation and data analysis software. Modern ITC instruments make it possible to measure heat effects as small as  $0.1 \mu\text{cal}$  ( $0.4 \mu\text{J}$ ), allowing the determination of binding constants,  $K_s$ , as large as  $10^8$ – $10^9 \text{ M}^{-1}$ .

Spink and Wadso (1976) published one of the first calorimetric studies of enzyme activity. Improvements in modern microcalorimeters including higher sensitivity, faster response, and the ability to make multiple additions of substrate (or inhibitors) has brought us to the point where ITC is now also routinely used to directly characterize the kinetic parameters ( $K_m$  and  $k_{\text{cat}}$ ) for an enzyme (Todd and Gomez, 2001; Williams and Toone, 1993). Kinetic studies take advantage of the fact that the calorimetric signal (heat rate, e.g.,  $\mu\text{cal}/\text{sec}$ ) is a direct measure of the reaction rate and the  $\Delta H$  for the reaction. Modern ITC instruments make it possible to measure heat rates as small as  $0.1 \mu\text{cal}/\text{sec}$ , allowing for the precise determination of reaction rates in the range of  $10^{-12}$  mol/sec. Values for  $K_m$  and  $k_{\text{cat}}$ , in the ranges of  $10^{-2}$ – $10^3 \mu\text{M}$  and  $0.05$ – $500 \text{ sec}^{-1}$ , respectively, can be determined by ITC.

Ladbury has published a series of annual reviews on ITC, describing the newest applications and a year-to-year survey of the literature on ITC applications (Ababou and Ladbury, 2006; Cliff *et al.*, 2004). In order to take full advantage of the powerful ITC technique, the user must be able to design the optimum experiment, understand the data analysis process, and appreciate the uncertainties in the fitting parameters. ITC experiment design and data analysis have been the subject of numerous papers (Bundle and Sigurskjold, 1994; Chaires, 2006; Fisher

and Singh, 1995; Freiere, 2004; Indyk and Fisher, 1998; Lewis and Murphy, 2005). This chapter reviews the planning of an optimal ITC experiment for either a binding or kinetic study, guides the reader through simulated sample experiments, and reviews analysis of the data and the interpretation of the results.

## II. Calorimetry Theory and Operation

### A. Heat Change Measurement and Theory

A calorimeter was one of the first scientific instruments reported in the early literature. Shortly after Black (1803) had measured the heat capacity and latent heat of water in the 1760s, Lavoisier designed an ice calorimeter and used this instrument to measure the metabolic heat produced by a guinea pig confined in the measurement chamber (1780s) (Lavoisier and Laplace, 1780; Fig. 1).

Thus, not only was a calorimeter the earliest scientific instrument but the first calorimetric experiment was a biologically relevant measurement.

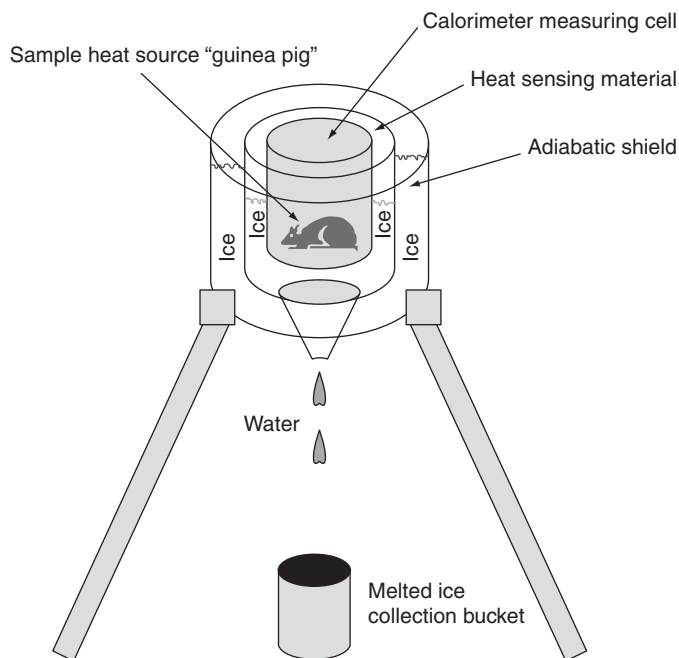


**Fig. 1** Lavoisier ice calorimeter used to measure the metabolic heat produced by a guinea pig confined in a measurement chamber. An external wooden layer surrounded a layer of ice that served as an adiabatic shield. Another separate layer of ice directly surrounded the central chamber. The water produced by melting this layer was measured to calculate the metabolic heat produced by the guinea pig.

Calorimetric measurements can be made in three different ways and commercial instruments are available which employ all three techniques. The three methods of measurement are (i) temperature change (either adiabatic or isoperibol), (ii) power compensation (often called isothermal), and (iii) heat conduction (Hansen *et al.*, 1985). It is important from the standpoint of experiment design, data collection, and data analysis to have a basic background in calorimeter design principles, especially from the standpoint of knowing what the raw signal data represent.

In a temperature change instrument, the heat produced (or consumed) by the reaction occurring in the calorimeter results in a change in temperature of the calorimeter measuring cell. The raw calorimetric signal is simply the temperature of the calorimeter cell as a function of time. With appropriate electrical or chemical calibration, the energy equivalent of the adiabatic (or isoperibol) calorimeter measuring cell can be determined. The measured temperature change is then converted to a heat change by simply multiplying the energy equivalent of the calorimeter,  $\epsilon_c$  (in cal/°C), times the measured temperature change,  $\Delta T$  in (°C).

In a power compensation instrument, the calorimeter measurement cell is controlled at a constant temperature (isothermal). This is accomplished by means of applying constant cooling to the cell and then using a temperature controller and heater to keep the cell temperature constant. As a chemical reaction takes place, any heat input from the chemical reaction is sensed and the power applied to the control heater reduced so that again the temperature remains constant. The heating power from the two sources, reaction and controlled heater, are obviously kept at a constant level so that a heat input from the reaction is compensated by a drop in the heat input from the controlled heater. The raw signal in the power compensation calorimeter is the power ( $\mu\text{cal}/\text{sec}$  or  $\mu\text{J}/\text{sec}$ ) applied to the control heater that is required to keep the calorimeter cell from changing temperature as a function of time. The heat change is then simply calculated by integrating the heater power over the time (sec) of the measurement (or more specifically the time required for the control heater power to return to a baseline value). A typical power compensation ITC is shown schematically in Fig. 2.

In a heat conduction calorimeter, the calorimeter measurement cell is passively maintained at a constant temperature by being coupled with heat flow sensors to a heat sink that is actively controlled at a constant temperature. The raw signal in the heat conduction calorimeter is typically a small voltage that is proportional to the very small  $\Delta T$  that is temporarily developed across the heat flow sensors as a result of the heat produced by the chemical reaction. The Lavoisier calorimeter mentioned earlier was essentially a heat conduction calorimeter with the inner ice layer being the heat flow sensor and the melted ice being the heat signal.

## B. Variations in Ligand/Macromolecule Mixing Techniques

A calorimetric experiment is begun by initiating a reaction within the calorimeter measuring cell. Historically, there have been three ways in which reagents have been brought together in the calorimeter. Other methods of initiating a reaction

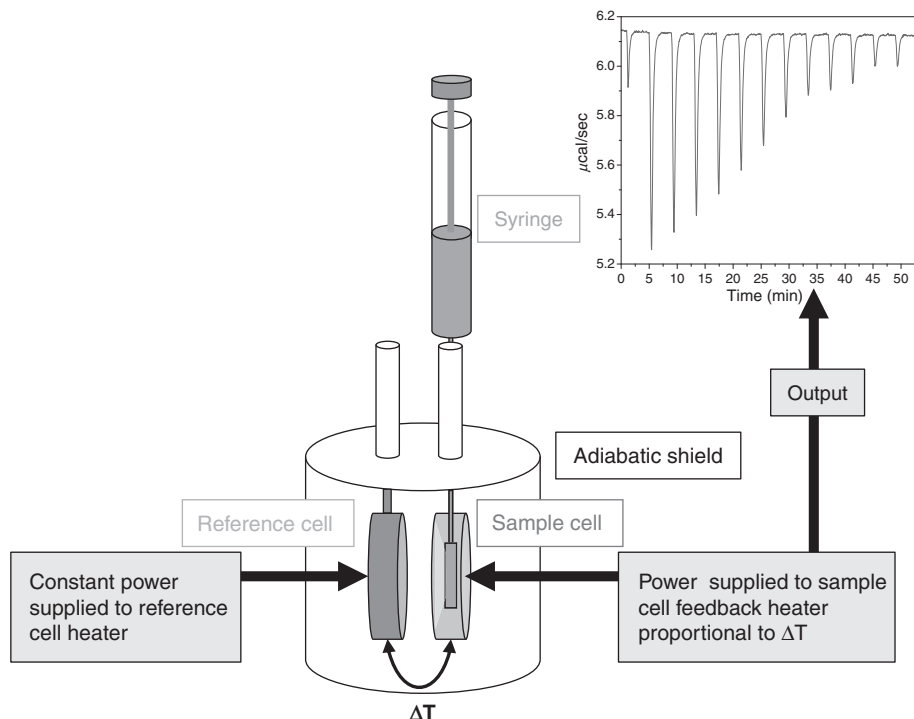


**Fig. 2** Representative diagram of a typical power compensation ITC. Major features of this type of instrument such as the reference and sample cells, syringe for adding titrant, and the adiabatic shield are noted in the figure. This diagram shows an oversimplification of how the power applied by the instrument to maintain constant temperature between the reference and sample cells is measured resulting in the instrument signal.

within the calorimeter have included temperature changes (either scanning  $T$  or a jump in  $T$ ) and pressure changes (either scanning  $P$  or a jump in  $P$ ). The three methods for bringing reagents in contact with one another include batch, titration, and flow methods (Hansen *et al.*, 1985). Batch methods have varied from rotating the whole calorimeter to mix the contents of two separate volumes in the batch cell, breaking an ampoule again resulting in the mixing of the ampoule contents with the contents of the rest of the calorimeter cell volume, and finally injecting a volume element from outside the cell into the volume contained within the calorimeter cell. Modern ITC instruments are often employed in a batch or a direct injection mode (DIE) in which a single larger injection of a reagent solution is made to start the experiment (e.g., kinetic measurements). More commonly, modern ITC instruments are used in a titration mode in which a number of incremental injections are made at time intervals in the course of a complete titration experiment. (The slow time response of the currently available ITC

instruments is such that continuous titration experiments are not possible.) Flow (and/or stopped flow) instruments having high enough sensitivity and fast enough response for most biological/biochemical studies are not currently available.

Each of the calorimeter types has its own advantages and disadvantages in terms of inherent sensitivity and time response. Adiabatic calorimeter designs are not used in the current crop of instruments designed for the study of biological systems. However, both power compensation and heat flow designs are in current use for these applications.

### C. Commercial Availability

“State-of-the-art” ITC (and DSC) instruments from both MicroCal<sup>®</sup> (MA) and Calorimetry Sciences Corporation<sup>®</sup> [CSC (UT)] use the power compensation measurement method. CSC also produces isothermal calorimeters using the heat conduction measurement technology that have higher sensitivity for slow reaction (e.g., kinetic and decomposition measurements). Product information, applications, measurement specifications, data analysis procedures, and bibliographies of recent calorimetric studies can be found at <http://www.calcorp.com/index.html> (Calorimetry Sciences Corporation<sup>®</sup>) and <http://www.microcal.com> (MicroCal<sup>®</sup>).

---

---

---

## III. Thermodynamic ITC Experiments

### A. Preface and Review of Basic Thermodynamics

A typical binding interaction between a ligand and a receptor molecule is illustrated in Fig. 3.

In biological terms, the ligand could be a substrate, inhibitor, drug, cofactor, coenzyme, prosthetic group, metal ion, polypeptide, protein, oligonucleotide, nucleic acid, or any one of a number of molecules thought (or known) to non-covalently interact with a specific site of a second molecule (typically a protein or nucleic acid). As noted in the figure, there are three species in equilibrium in

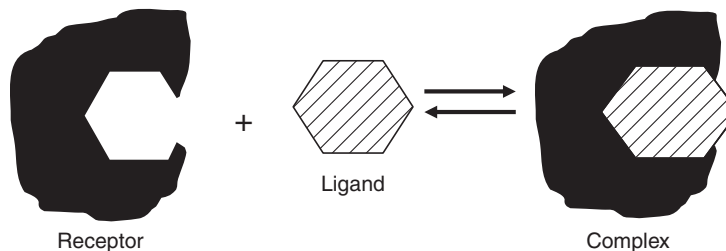


**Fig. 3** A simplified model of a typical receptor/ligand-binding interaction. The ligand in this representation is shown to geometrically match the binding site on the receptor to indicate a specific binding interaction.

solution. They are the biopolymer with a vacant binding site, the free ligand, and the complex. A fundamental understanding of the pictured interaction would require at a minimum knowledge of the equilibrium constant for the binding process,  $K$ , and the binding stoichiometry,  $n$  (how many ligands are there bound to the macromolecule at saturation). A richer understanding of the ligand macromolecule interaction is established if the enthalpy ( $\Delta H$ ) and entropy ( $\Delta S$ ) change contributions to the formation of the complex are known. The following equations are provided as a brief review of the relevant thermodynamic relationships:

$$K_{\text{eq}} = \left\{ \frac{[\text{Complex}]}{[\text{Receptor}]} \times [\text{Ligand}] \right\}_{\text{equilibrium}} \quad (1)$$

$$\Delta G^\circ = -RT \ln K_{\text{eq}} \quad (2)$$

$$\Delta G = \Delta G^\circ + RT \ln \left\{ \frac{[\text{Complex}]}{[\text{Receptor}]} \times [\text{Ligand}] \right\}_{\text{actual}} \quad (3)$$

$$\Delta G = \Delta H - T\Delta S \quad (4)$$

where  $K_{\text{eq}}$  ( $K$ ) is the equilibrium constant,  $[X]$  is the molar equilibrium (or actual) concentration of species  $X$ ,  $\Delta G^\circ$  is the standard Gibbs free energy change,  $R$  is the universal gas constant,  $T$  is the temperature in Kelvin,  $\Delta G$  is the actual Gibbs free energy change,  $\Delta H$  is the enthalpy change, and  $\Delta S$  is the entropy change for complex formation. The unique advantage of the ITC experiment is that it is possible in a single experiment, if done under optimum conditions, to obtain accurate values for  $K$  (or  $\Delta G$ ),  $\Delta H$ ,  $-T\Delta S$ , and  $n$ , where  $n$  is the stoichiometry of the interaction (mol ligand/mol complex).

What do we mean by optimum conditions? The ITC experiment must be done under conditions where the heat change is both measurable for each injection and where the heat change varies for subsequent injections producing a curved thermogram (a plot of heat change vs injection number, or mol ratio of ligand/macromolecule). The first condition is obvious, the instrument is a calorimeter and if there are insufficient calories produced by the reaction, then the experiment will be impossible. The second is more problematic since the curvature in the thermogram is a function of the concentration of the macromolecule,  $[M]$ , and the equilibrium constant  $K$ . Figure 4 illustrates this point in that the two sets of panels with identical Brandt's "c" parameters ( $c = 10$  in Fig. 4A and B, and  $c = 100$  in Fig. 4C and D) (Wiseman *et al.*, 1989) exhibit the same curvature. The Brandt's "c" parameter is defined to be equal to the total macromolecule concentration

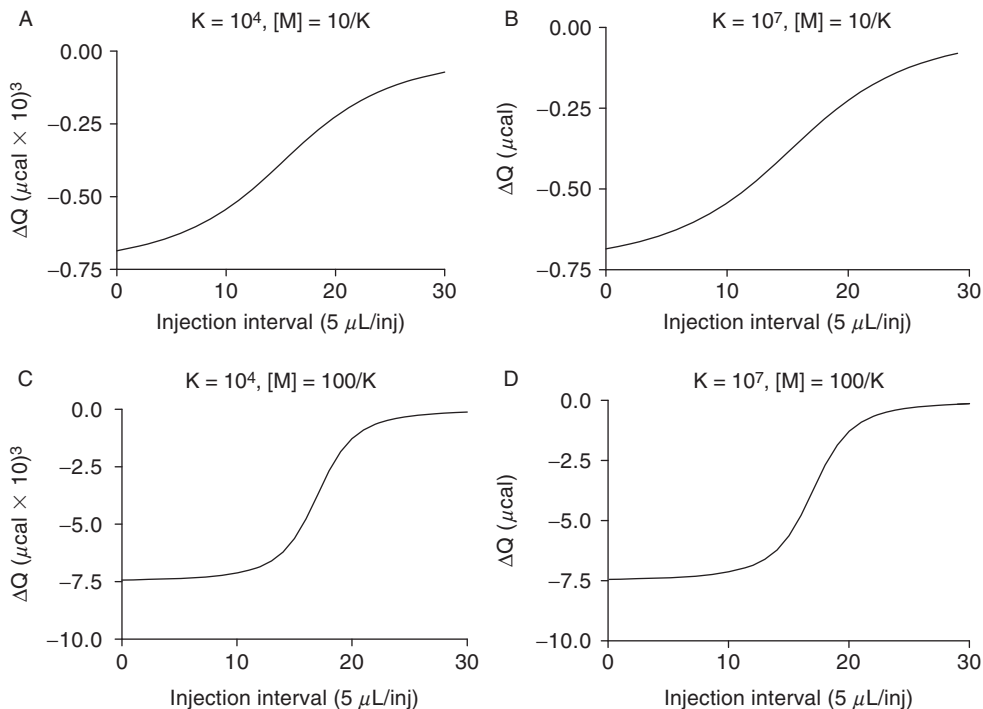


**Fig. 4** Four plots demonstrating the relationship between curvature and experimental concentrations. The two top panels (A and B) are simulated with a “ $c$ ” parameter of 10, and the two bottom panels are simulated with a “ $c$ ” parameter of 100. Panels A and C represent a system with a fairly low  $K$  value of  $1 \times 10^4$ , while panels B and D represent a system with a more robust  $K$  value of  $1 \times 10^7$ .

multiplied by the equilibrium constant ( $c = [M_{\text{tot}}] \times K$ ). Each of the panels in Fig. 4 exhibits a thermogram with acceptable curvature for the nonlinear regression analysis required to obtain an accurate value for  $K$ . However, the experiment depicted in panel B does not produce enough heat ( $<0.5 \mu\text{cal}$  for the largest heats), while the experiment depicted in panel C produces too much heat ( $>8000 \mu\text{cal}$  for the largest heats) to yield data sets that are optimal for the determination of the thermodynamic parameters  $K$ ,  $\Delta H$ , and  $n$ . Obviously, experiments with reactions having a very large equilibrium constant ( $K > 10^8 \text{ M}^{-1}$ ) need to be done at low macromolecule concentrations to produce the required curvature in the thermogram but at high enough concentrations to produce measurable heats. The reverse is true for weak complexes ( $K < 10^4 \text{ M}^{-1}$ ) in that here the problem is to achieve macromolecule concentrations where the curvature is appropriate but where the heats are not too large to be accurately measured.

There are several steps to running the ITC experiment. These are (i) planning the experiment (e.g., simulations), (ii) preparing the ligand and macromolecule solutions, (iii) collecting the raw ITC data, (iv) collecting the blank (ligand solution

dilution), (v) correcting the raw ITC data, (vi) nonlinear regression of the corrected titration data to provide estimates of the thermodynamic parameter values, and (vii) interpretation of the model data. Each step will be discussed in turn below for an example ITC experiment. In our discussions of running a typical ITC experiment, we will use the binding of a hypothetical ligand, L, to a hypothetical protein, P. The approximate thermodynamic parameters for the simulated system are  $K \approx 1 \times 10^5 \text{ M}^{-1}$ ,  $\Delta H \approx -10 \text{ kcal/mol}$ , and with a stoichiometry of 1:1 at 25 °C. (The data and analysis shown in subsequent sections have been simulated for clarity.)

## B. Planning the Thermodynamic ITC Experiment

The first step in running the ITC experiment is to determine the concentrations for the macromolecule and ligand solutions. If the objective of the ITC experiment is only to determine the binding enthalpy change,  $\Delta H$ , then the only consideration is that the concentration of the ligand will be large enough that an accurately measurable heat effect,  $\geq 10 \mu\text{cal}$ , will be observed and that the macromolecule concentration will be in excess. In the case of our hypothetical system, these conditions would be met with  $[\text{L}] = 2 \times 10^{-4} \text{ M}$ , and  $[\text{P}] = 1.7 \times 10^{-4} \text{ M}$ . With an injection volume of  $5 \mu\text{l}$ , the heat per injection would be given by Eq. (6), and there would be no curvature in the thermogram:

$$Q_{\text{inj}} = (\Delta H \times [\text{L}] \times V_{\text{injection}}) \quad (5)$$

$$Q_{\text{inj}} = (-10 \text{ kcal mol}^{-1}) \times (2 \times 10^{-4} \text{ M}) \times (5 \times 10^{-6}) \quad (6)$$

If the concentrations of the ligand,  $[\text{L}]$ , were increased to  $5 \times 10^{-3} \text{ M}$ , the thermogram would show curvature similar to that shown in the upper panel of Fig. 4 ( $c = 10$ ) and an endpoint would be reached after  $\sim 20$  ( $5 \mu\text{l}$ ) injections. The integrated heat values for the first injections would now be over  $-500 \mu\text{cal}$ . Increasing the concentration of the protein,  $[\text{P}]$ , to  $1.7 \times 10^{-3} \text{ M}$  ( $c = 100$ ) and the ligand concentration to  $5 \times 10^{-2} \text{ M}$  or so would yield a thermogram showing the same curvature as that shown in the lower panels of Fig. 4. In this last case, the heat observed in the early injections would be too large, over  $-5000 \mu\text{cal}$ . Figure 5 shows simulated ITC data for an experiment done under the second set of conditions ( $c = 10$ ) where both  $K$  and  $\Delta H$  would be well determined.

## C. Running the Thermodynamic ITC Experiment

### 1. Solution Preparation and Handling

Now that we know the desired concentrations for the macromolecule and the ligand solutions, let us discuss solution preparation and handling. First, since the final results of the ITC experiment depend on exact knowledge of the titrate and titrant solution concentrations, it is imperative that the concentrations be made as

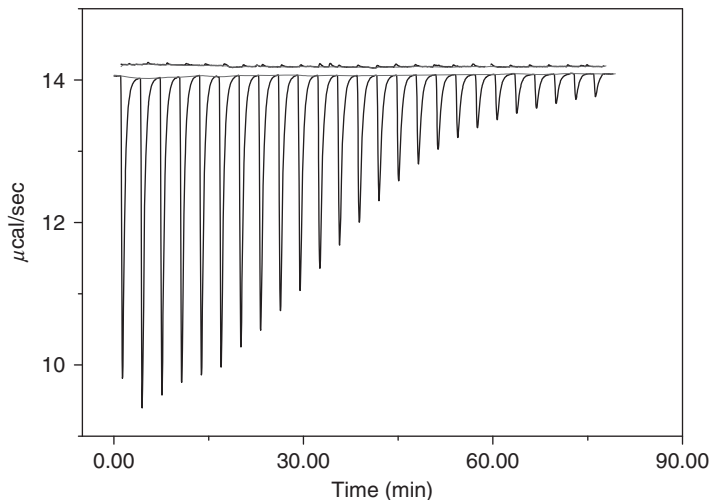


**Fig. 5** Simulated ITC Raw Data showing the instrument response for a power compensation ITC instrument. The simulated data represent an exothermic reaction at concentrations producing a reasonable amount of curvature. Above the simulated “experimental” data is a smaller data set representing a typical “instrument blank.”

accurately as possible. Perhaps the ITC solutions can be made by volumetric dilution of stock solutions that were made up by weight. Whenever possible the concentrations should be verified by another analytical procedure (e.g., absorbance, kinetic activity, or other analysis).

It is extremely important that the two solutions be matched with regard to composition, for example, pH, buffer, and salt concentration. If the two solutions are not perfectly matched, there may be heat of mixing (or dilution) signals that overwhelm the heat signals for the binding reaction. It is typical that the solution of the macromolecule is exhaustively dialyzed against a large volume of the buffer. The artifact heats of mixing can be minimized by using the dialysate from preparation of the macromolecule solution as the “solvent” for preparation of the ligand solution.

## 2. Collecting the Raw ITC Data

ITC data collection involves proper identification of optimal experimental run parameters (these should be roughly the same parameters used when simulating data to determine optimal concentrations). The number of injections required for an experiment varies. The number and volume of injections should be adjusted depending on the region of the isotherm that requires the most resolution (using the same concentrations, a titration programmed to deliver a larger number of

injections of a smaller volume will result in a better nonlinear regression fit since there are more points included in the titration).

### 3. Correcting the Raw ITC Data

Obviously, the dialysis/dialysate approach will virtually eliminate the mixing or dilution effects for all solute species in common between the macromolecule and ligand solutions. The exception is that the heat of dilution for the ligand itself must be measured in a blank experiment. In this blank experiment, the ligand solution is titrated into buffer in the sample cell. The heat of dilution of the macromolecule should also be measured in a second blank experiment. This is done by simply injecting buffer from the syringe into the macromolecule solution in the sample cell. Usually the heat of dilution of the macromolecule measured in this way is negligible. To be completely rigorous, a third blank experiment should also be done. This buffer into buffer experiment may be thought of as an instrument blank. The equation to correct the heat data for dilution effects is

$$Q_{\text{corr}} = Q_{\text{meas}} - Q_{\text{dil,ligand}} - Q_{\text{dil,macromolecule}} - Q_{\text{blank}} \quad (7)$$

The blank corrections are for the same injection volumes as used in the collection of the actual titration data. In the case of the ligand/protein titration experiment shown in Fig. 5, the only significant correction is for the dilution of the titrant (the results of the ligand dilution blank experiment are also shown in Fig. 5).

Another complicating reaction encountered in many biological binding experiments results from the release (or uptake) of protons as binding occurs. The released protons are taken up by the buffer conjugate base. The correction for this complicating reaction requires knowledge of the number of protons released (or taken up) and the heat of ionization of the buffer. The equation to correct for the ionization of the buffer is

$$Q_{\text{corr}} = Q_{\text{meas}} - (\Delta H_{\text{ion}} \times n_p) \quad (8)$$

where  $\Delta H_{\text{ion}}$  is the heat of proton ionization for the buffer and  $n_p$  is the number of protons released on binding 1 mol of ligand. Since  $n_p$  is typically unknown, this correction would be accomplished by titrations done in two buffers with different heats of ionization. In this case, the complication actually yields additional information regarding the binding reaction. This phenomenon also provides an approach to manipulating the heat signal for a reaction that is accompanied by proton release. By simply using a buffer with a large heat of ionization, the heat signal can be enhanced. Alternatively, the use of a buffer with a small heat of ionization ( $\Delta H_{\text{ion}} \approx 0$ ) could be used to minimize the ‘‘artifact signal.’’ To determine an optimal buffer for your system, the heats of ionization (or protonation) of various buffer solutions can be found in references [Christensen \*et al.\* \(1976\)](#) and [Fasman \(1976\)](#).

Finally, since the generation of bubbles in the sample (or reference) solutions during an ITC experiment will generate spurious heat signals, the solutions should be degassed prior to filling the cell and injection syringe. The ITC manufacturers provide vacuum degassing accessories for this purpose. Precautions need to be taken to avoid boiling the solutions and changing the concentrations. Also ITC manufacturers supply cell loading syringes and instructions on cell filling that should be followed to avoid the problem of introducing bubbles.

#### 4. Example ITC Experiment

The example ITC experiment described is for the binding of our hypothetical ligand, L, to our hypothetical protein, P, the same experiment that was shown in Fig. 5. In the hypothetical experiment, both the ligand and protein were purchased from commercial sources (e.g., Sigma-Aldrich, St. Louis, MO) and used without further purification. The protein solution was prepared by dissolving a weighed amount of the lyophilized powder in acetate buffer and then dialyzed for 16 h at 4 °C against 4 liter of acetate buffer using 3500 MWCO Spectrofluor dialysis tubing. The ligand solution was prepared by dissolving a weighed amount of the pure compound in the acetate buffer dialysate. The final concentrations for both the protein and ligand were determined by the appropriate analytical procedure (e.g., a spectrophotometric assay). Both the titrate and titrant solutions were degassed prior to loading the calorimeter cell and injection syringe.

The ITC experiment was run at 25 °C and was set to deliver 25 (5  $\mu$ l) injections at 300-sec intervals. The raw ITC data are shown in Fig. 5. Data are shown for one titration experiment in which the ligand solution was added to the protein solution in the cell, and one titrant dilution experiment in which the ligand solution was added to buffer (dialysate) in the cell. The dilution of the titrant is slightly endothermic and contributes less than +0.6  $\mu$ cal to the total heat observed for the addition of 5  $\mu$ l of ligand in the protein titration. The titrant dilution represents less than 0.5% of the heat signal observed for the initial titrant additions. The dilution experiment in which buffer was added to the protein solution in the cell is not shown since the heat of dilution of the protein was even less significant than the ligand dilution under the conditions of these experiments.

The dilution-corrected and integrated heat data are shown in Fig. 6. The integrated heat data were fit with a one-site binding model using the Origin-7™ software provided with the MicroCal VP-ITC. The “best-fit” parameters resulting from the nonlinear regression fit of these data are also shown in Fig. 6 along with the fitted curve. The  $K$  and  $\Delta H$  values determined in this experiment would be the appropriate values for the experiment performed under the stated conditions of temperatures, salt concentrations, buffer of choice, and at the specified pH. A more detailed discussion of the nonlinear regression fitting and data interpretation follows.

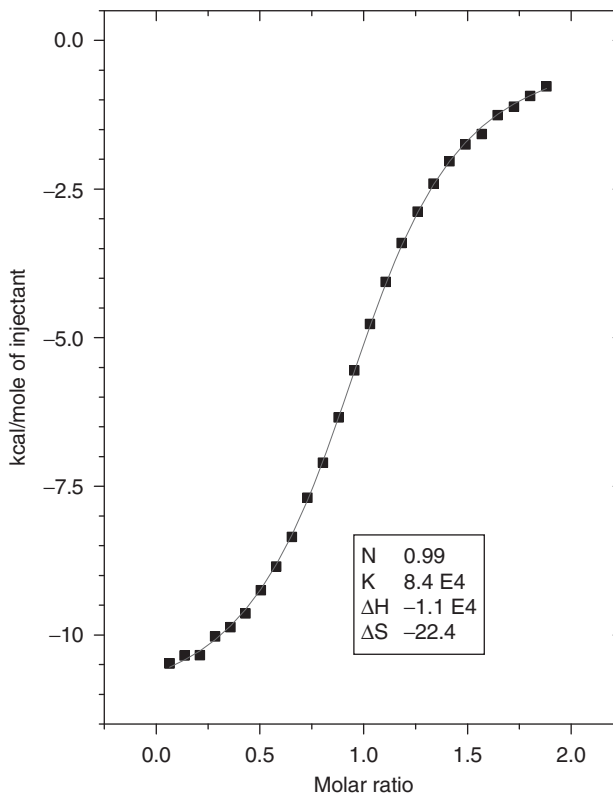


**Fig. 6** Simulated data set representing the integration of the raw data shown in Fig. 5. This data has been corrected by subtraction of appropriate blank experiments and then fit with nonlinear regression. The “best-fit” parameters are given in the box in the lower right-hand corner of the plot.

#### D. Analyzing Thermodynamic Data

In order to analyze ITC data for the relevant thermodynamic parameters, a binding model must first be assumed [e.g., one-site (or  $n$  identical sites), two independent sites, or sequential binding]. The analysis of the thermogram is a curve fitting process in which a nonlinear regression procedure is used to fit a model to the data. The model is a mathematical description of a physical, chemical, or biological process that is taking place in the calorimeter and in which the dependent variable (e.g., heat or heat rate) is defined as a function of the independent variable (e.g., moles of titrant added) and one or more model parameters. In the case of binding experiments, the model is formed from the equilibrium constant and mass balance equations. Nonlinear regression is used along with the model equations to determine the best values of the fitting parameters (e.g.,  $K$ ,  $\Delta H$ , and  $n$ ). The goal is to model the experimental data within expected experimental error, using the simplest model, and a model that makes sense in the light of what is

already known about the system (e.g., stoichiometry). The model should help to understand the actual chemistry, biology, or physics of the system being studied. It is important to note that one of the authors of this chapter has often said “All models are wrong, but some are useful.”

The nonlinear regression analysis of ITC data is an iterative process. The first step in the process is to make initial estimates for each of the parameters in the model equation. Using these values, a fit or theoretical curve is generated and then compared to the actual data curve. An error function is calculated that is the sum of the squared deviations between the data and the model curve. An accepted algorithm is then used to adjust the fit parameters to move the calculated curve closer to the data points. This process is repeated over and over until the error function is minimized or insignificantly changes with subsequent iterations. If the error function cannot be minimized to an acceptable value, that is, an error square sum that is consistent with the expected experimental error, then another model must be tried. It is important to note here that “the best-fit” parameter values may depend on the starting estimates chosen in the first step or on the stopping criteria of the last step.

Figure 5 shows the raw ITC data for the hypothetical ligand protein titration, while Fig. 6 shows the integrated heat data along with a nonlinear regression fit to a one-site binding model. The line through the data points corresponds to the theoretical heat produced for 1:1 complex formation between the ligand and the protein and the best-fit values for the parameters  $K$ ,  $\Delta H$ ,  $\Delta S$ , and  $n$  are listed in the box in the lower right corner of the plot. The nonlinear regression analysis shown was performed using the simulated data in Fig. 5 and the one-site reaction model in the Origin 7 ITC software package provided by the ITC manufacturer, in this case MicroCal. Both Calorimetry Sciences and MicroCal provide for more complex binding models in their software packages, for example, single set of identical sites, two sets of independent sites, sequential and binding. They have also made it possible for the experienced user to add models within limits (i.e., the mathematics engine in Origin is unable to solve polynomials higher than third degree). In order to better understand the nonlinear regression (or curve fitting) analysis of ITC data, we will first discuss the “one-site” model in more detail.

The thermogram generated in the ITC experiment is a simple summation of all of the heat-producing reactions that occur as an aliquot of titrant is added. The initial heats are larger than the heats for subsequent additions since at the beginning of the titration there is a large excess of empty or unpopulated binding sites. Initial heats most typically are the result of complete reaction of the added ligand. As the titration proceeds, less and less of the added ligand is bound and there are three species existing in solution: free ligand, unoccupied binding sites, and the ligand/protein complex. The heat produced in the ITC experiment is linearly dependent on the  $\Delta H$  or the reaction and nonlinearly dependent on the  $K$ .

The ITC thermogram for a generic binding process is modeled by Eqs. (9) and (10) (Eatough *et al.*, 1985; Freyer *et al.*, 2006, 2007a,c; Lewis and Murphy, 2005).

$$\Theta_j = \frac{[L]K_j}{1 + [L]K_j} \quad (9)$$

$$L_t = [L] + P_t \sum_{j=1}^k (n_j \Theta_j) \quad (10)$$

Equations (9) and (10) describe the equilibrium and mass balance relationships for the system being studied, where  $\Theta_j$  is the fraction of site  $j$  occupied by ligand,  $L_t$  is the total ligand concentration,  $[L]$  is the free ligand concentration,  $P_t$  is the total macromolecule concentration,  $K_j$  is the binding constant of process  $j$ , and  $n_j$  is the total stoichiometric ratio for process  $j$ . Each of the equations is defined for all potential binding sites, and solutions for any multiple site binding process can be defined. Substituting (9) into (10) and expanding the polynomial in terms of the indeterminate  $[L]$  results in a  $(k + 1)$  degree polynomial. Thus, in order to determine a solution for a one-site-independent binding process, roots of a second degree polynomial must be found. Substitution of  $[L]$  into Eq. (9) allows the fraction of binding site  $j$  that is occupied to be calculated.

$$Q = P_t V_0 \left( \sum_{j=1}^k n_j \Theta_j \Delta H_j \right) \quad (11)$$

$$\Delta Q(i) = Q(i) - Q(i - 1) \quad (12)$$

The total heat produced can be calculated from Eq. (11), where  $V_0$  is the initial volume of the sample cell and  $\Delta H_j$  is the molar enthalpy change for process  $j$ . The differential heat is defined by Eq. (12), where  $i$  represents the injection number. Nonlinear regression was performed on the parameters  $K_1$ ,  $n_1$ , and  $\Delta H_1$  to obtain a best fit to the experimental data shown in Figs. 5 and 6. The good news is that this whole curve fitting process is transparent to the beginning or casual user of the ITC technique. It is only when more complex models are required to fit the binding data that the process becomes much more difficult.

There are many nonlinear regression algorithms available but all result in almost the same answer. In Fig. 7, we present a 3-D plot of the error square sum surface that one would expect to get from a one-site analysis. The  $z$ -axis represents the square of difference between experimental and theoretical points, the  $x$ -axis the log of the equilibrium constant  $K$ , and the  $y$ -axis the value for  $\Delta H$ . It is easy to see that the minimum in the error function is at the bottom of the net. This best result is unambiguous in that single values of  $K$  and  $\Delta H$  are found that yield the smallest error.

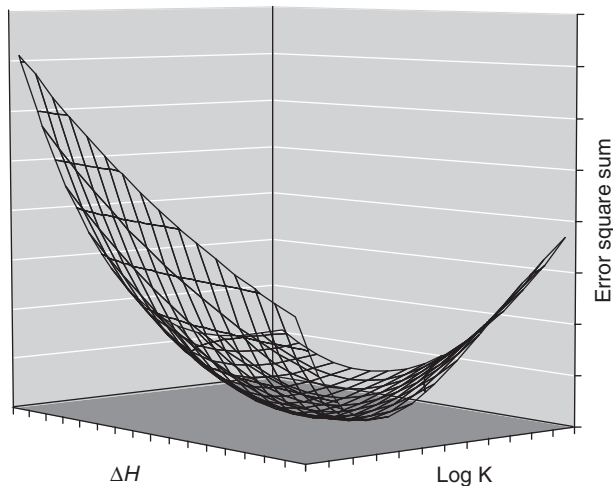


**Fig. 7** Error square sum surface for a typical “one-site” nonlinear regression fit. “Best-fit” parameters for a given nonlinear regression will lie in the minimum of the error surface. Searching along the gridlines (2-D parabolas) would be useful in generating confidence intervals (see Chapter 24 by Johnson, this volume).

There are several chapters in this volume that discuss ligand-binding reactions, experimental techniques other than ITC, and data fitting in general. The information in these chapters is complimentary to the discussions of ligand binding and data fitting presented in this chapter. See for example, Chapter 1 by Garbett and Chaires, Chapter 24 by Johnson, Chapter 23 by Tellinghuisen, and Chapter 3 by Fariál *et al.*, this volume.

### E. Models

The equilibrium constant and mass balance expressions for the one-site ( $n$  identical sites), two-site (two independent sites), and sequential sites models are defined differently as shown below:

One-set (or  $n$  identical sites):

$$K = \frac{\Theta}{(1 - \Theta) \cdot [L]} \quad (13)$$

Two sets of independent sites:

$$K_1 = \frac{\Theta_1}{(1 - \Theta_1) \cdot [L]} \quad \text{and} \quad K_2 = \frac{\Theta_2}{(1 - \Theta_2) \cdot [L]} \quad (14)$$

Sequential sites:

$$K_1 = \frac{[\text{PL}]}{[\text{P}][\text{L}]}, K_2 = \frac{[\text{PL}_2]}{[\text{PL}][\text{L}]}, \text{ and } K_3 = \frac{[\text{PL}_3]}{[\text{PL}_2][\text{L}]} \quad (15)$$

$$L_t = [\text{L}] + [\text{PL}] + 2[\text{PL}_2] + 3[\text{PL}_3] \quad (16)$$

$$P_t = [\text{P}] + [\text{PL}] + [\text{PL}_2] + [\text{PL}_3] \quad (17)$$

These models are addressed in the analysis software provided by CSC<sup>®</sup> Bindworks<sup>™</sup> and MicroCal<sup>®</sup> ITC Origin<sup>™</sup>. More complicated models, for example, three independent sites or fraction-sites would require the user to write their own analysis routines.

Theoretical ITC thermograms are shown in Fig. 8 for three different systems in which 2 mol of ligand are bound to two independent binding sites on the macromolecule.

In the upper panel, the thermogram looks as if there might be either two independent or two identical sites, each described by a similar value for  $K$  and  $\Delta H$ . In reality, we can only determine the weakest value for  $K$  and a single of  $\Delta H$  value for both sites ( $\Delta H_1$  and  $\Delta H_2$  must be equal) in this system. If we look at the middle panel in the figure, we can see that again the total binding stoichiometry is 2:1, but the more tightly bound ligand also has the most exothermic enthalpy change. In the lower panel, we show a simulation for two independent sites in which the weaker binding process has the more exothermic  $\Delta H$ .

Let us move on to a slightly more complicated three-site simulation as shown in Fig. 9.

Although perhaps not immediately obvious, there are three different binding processes present in the data set shown. The highest affinity process has the largest exothermic  $\Delta H$ , while the next two processes have overlapping  $K$  values and decreasing values for their  $\Delta H$  values. The line through the simulated data points represents the nonlinear fit to the data. The best-fit values returned from the nonlinear regression analysis were within experimental error of the values used to generate the simulated data.

## F. Error Analysis/Monte Carlo

The statistical significance of the best-fit parameters is always a matter of concern. It is important to know that the model parameters reported are actually meaningful. This becomes more of a concern as the models get more complicated and the number of fitting parameters increases. One way in which the certainty of the parameters can be tested is to perform a Monte Carlo analysis. In order to give the reader confidence in the fitting of ITC data to yield a large number of

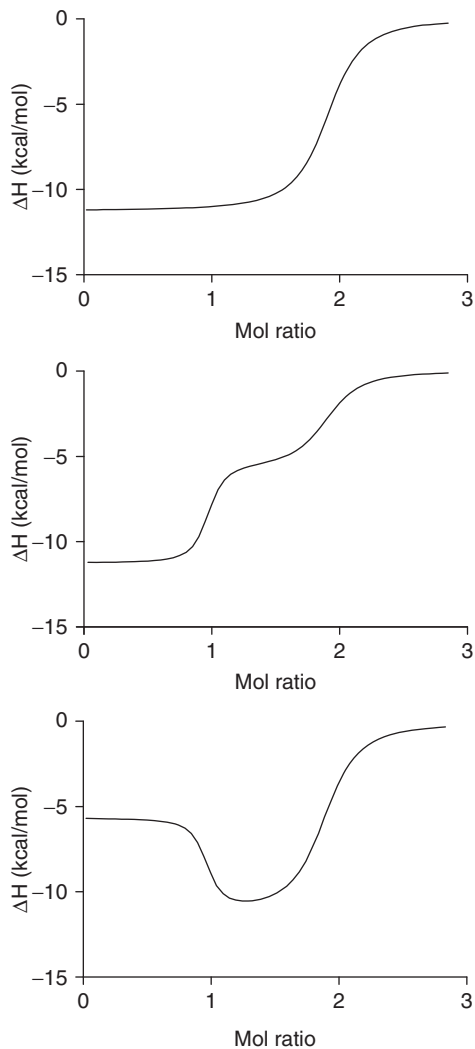


**Fig. 8** Representation of three possible experimental observations for a system where two ligand molecules bind to a receptor molecule. In all three cases, the stoichiometry demonstrates that two ligand molecules are binding to the receptor molecule. The top panel represents a system where the enthalpy change and binding affinity for both ligands are close enough to be thermodynamically indistinguishable. The middle panel represents a system where the binding site with higher affinity is accompanied by a more exothermic enthalpy change. The bottom panel represents a system where the higher binding affinity site demonstrates a less exothermic enthalpy change than the lower binding affinity site.

thermodynamic parameters, we performed a Monte Carlo analysis on the simulated three-sites data shown in Fig. 9. A Monte Carlo analysis is equivalent to running a very large number of actual experiments and then comparing the

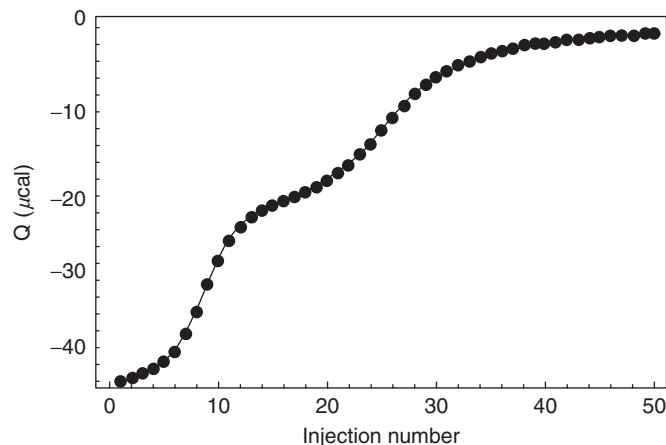


**Fig. 9** A simulated plot representing a system where there are three ligand molecules binding to a receptor molecule. The highest affinity binding site has the largest exothermic enthalpy change, while the binding affinity and enthalpy changes for binding ligands to the other two binding sites are indistinguishable.

results of the fits from this large number of experiments. In our Monte Carlo analysis of the three-sites data set, we ran the equivalent of 1000 ITC virtual experiments. The Monte Carlo procedure involves several steps: (i) the generation of a perfect data set (see Fig. 9), (ii) adding random (Gaussian) noise correlated to instrumental error to the data, (iii) performing the three-sites nonlinear regression on the noisy virtual data set, and (iv) repeating the virtual experiment 1000 times. The noise level employed in this analysis was  $\pm 0.25 \mu\text{cal}$ s, which is the expected error in ITC measured heat values. This error was randomly Gaussian and added to each point in the “perfect” data set. The 1000 sets of “best-fit” parameters were placed into a statistical program and the distributions analyzed to determine the statistical error of each parameter. Table I lists the values of  $K_j$  and  $\Delta H_j$  that were used to generate the perfect data set (Fig. 9) and the values that were returned from the Monte Carlo analysis described above.

Clearly, the three-sites model (and other complex models) can be applied to ITC and the nonlinear regression can yield best-fit parameters with high levels of certainty. There are a number of ways to view the parameter distributions from a Monte Carlo analysis and in Fig. 10 we show a Saroff Plot in which the listed parameter is changed over a range of values and the nonlinear regression performed on the remaining parameters.

While it is obvious that some parameters are better determined than others (e.g.,  $K_1$ ,  $K_2$ ,  $\Delta H_1$ ,  $\Delta H_2$ , and  $n_3$ ), and some are cross correlated, most show a clearly defined minimum in the error function and thus are well determined, although the error bars may not be symmetric. The cross correlation of parameters can be visualized by plotting one parameter versus another as described by Correia and Chaires (1994).

**Table I**  
**The Results of Monte Carlo Analysis of the Simulated “Three-Sites”**  
**Data Shown in Fig. 9**

Parameter	Model value	Calculated value
$K_1$	$5.0 \times 10^7$	$5.02 \times 10^7 \pm 3.5 \times 10^6$
$K_2$	$1.0 \times 10^6$	$1.008 \times 10^6 \pm 7.9 \times 10^4$
$K_3$	$3.0 \times 10^4$	$3.02 \times 10^4 \pm 3.0 \times 10^3$
$\Delta H_1$	-10 kcal/mol	$-10 \pm 0.04$ kcal/mol
$\Delta H_2$	-5 kcal/mol	$-5.0 \pm 0.05$ kcal/mol
$\Delta H_3$	-2 kcal/mol	$-2.0 \pm 0.12$ kcal/mol

Column 2 relates the “best-fit” parameters for fitting the simulated data, and column 3 shows the result of the Monte Carlo analysis 1000 simulated experiment average  $\pm 1$  standard deviation.

## G. Summary

The ITC method for the simultaneous determination of  $K$  and  $\Delta H$  is certainly an important technique for the characterization of biological binding interactions. The emphasis of this chapter was to guide users new to the technique through the process of performing an ITC experiment and to point out that care must be taken both in the planning of the experiment and in the interpretation of the results. The conclusions that can be drawn from the above discussions of the ITC-binding experiment, the nonlinear fitting of ITC data, and data interpretation are listed below.

- It is important in planning the ITC-binding experiment that reasonable concentrations be chosen for the macromolecule and the ligand. This is most easily done by simulating the thermogram with reasonable guesses for  $K$  and  $\Delta H$  (although the guess for  $\Delta H$  is less critical).
- The linear parameters  $\Delta H$  and  $n$  will be better determined than the nonlinear parameter  $K$ .
- The best results will be obtained at  $10/K \leq [M] \leq 100/K$ , and  $[L] \approx 20\text{--}50 \cdot [M]$ , subject to solubility and heat signal considerations.
- The best results will be obtained when the initial integrated heat(s) are larger than  $10 \mu\text{cal}$ .
- The number of points in the titration is not critical as long as the collection of more points does not reduce the measured heat to the point where random error in the  $\partial q$  values becomes significant.
- Fitting for the fewest number of parameters is always helpful in reducing the uncertainty in the fitted parameters, for example, constrain  $n$  to fit for  $\Delta H$  and  $K$ , or constrain  $\Delta H$  and  $n$  to fit for  $K$ .
- Titrant and titrate concentrations must be accurately known. (Nonintegral values for  $n$  are often the result of concentration errors. Errors in titrate concentration contribute directly to a similar systematic error in  $n$ . Errors in titrant concentration or titrant delivery contribute directly to similar errors in  $\Delta H$ .)

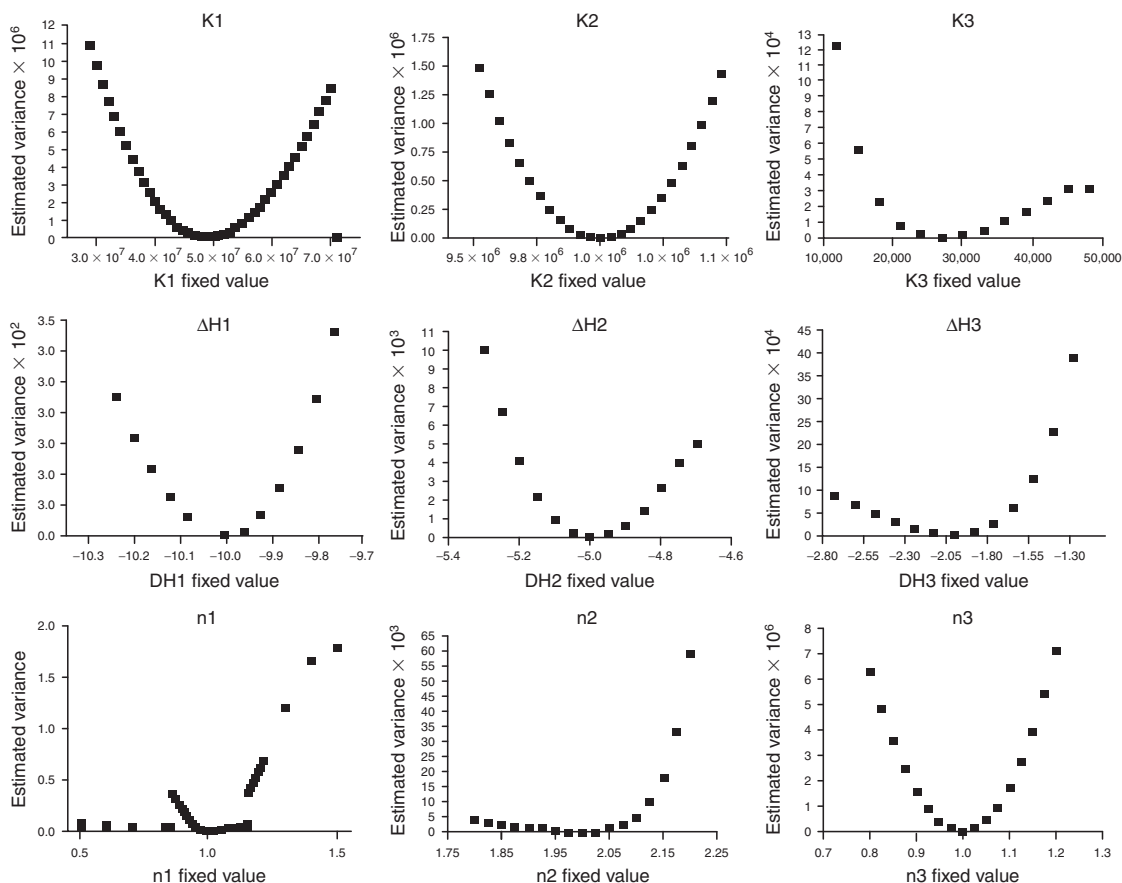


**Fig. 10** Saroff distribution of error generated from the Monte Carlo analysis performed on the simulated data given in Fig. 9. These plots show the distribution of error in each of the nine fitting parameters demonstrating that some parameters can be better determined than others.

## IV. Kinetic ITC Experiments

### A. Reaction Rate Versus Heat Rate

A typical enzyme substrate interaction is illustrated in Fig. 11.

In biological terms, ligands of interest other than the normal substrate could be inhibitors, cofactors, coenzymes, prosthetic groups, metal ions, or other small molecules. However, since the point of these experiments is to probe the kinetics and means by which substrate is converted to product, the typical experiment involves enzyme, substrate, and possibly other reactants involved in the enzyme-catalyzed reaction. One difference, in comparison to the binding experiments,

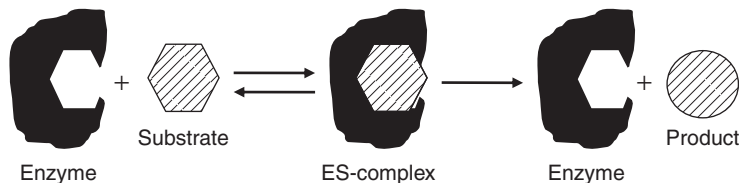


**Fig. 11** A simplified model of a typical enzyme/substrate interaction. The substrate in this representation is shown to geometrically match the active site of the enzyme to indicate a specific interaction. The substrate is then converted to product leaving a regenerated enzyme.

is that the enzyme-catalyzed heats of reaction are usually much larger than the heats observed for noncovalent binding interactions. A fundamental understanding of the pictured reaction would require at a minimum knowledge of the Michaelis constant,  $K_m$ , and the turnover number,  $k_{cat}$ . Again a richer understanding of the enzyme-catalyzed reaction would be established if the substrate-binding constant (not exactly the same as  $1/K_m$ ), the enthalpy change,  $\Delta H$ , for the reaction ( $S \rightarrow P$ ), and any mechanistic information (e.g., hyperbolic vs sigmoidal dependence on  $[S]$ , response to various types of inhibitors, effects of temperature, pH, or other solution conditions) were known. The ITC experiment can provide information in all of these areas. The following equations are provided as a review of the relevant kinetic relationships:



$$K_m = \frac{(k_{-1} + k_2)}{k_1} \quad (19)$$

$$K_{eq} = \frac{[ES]}{[E][S]} \approx \frac{1}{K_m} \quad (20)$$

$$k_{cat} = \frac{v_{max}}{[E]_t} \quad (21)$$

$$v_0 = v_{max} \frac{[S]}{(K_m + [S])} = \frac{k_{cat}[E]_t[S]}{(K_m + [S])} \quad (22)$$

where  $k_1$ ,  $k_{-1}$ , and  $k_2$  are the rate constants for the forward and reverse reactions in the reaction scheme,  $K_m$  is the Michaelis constant,  $K$  is the binding constant,  $k_{cat}$  is

the turnover number,  $v_0$  is the initial velocity,  $v_{\max}$  is the maximal velocity (when  $[ES] = [E]_t$ ), and  $[X]$  is the molar concentration of species  $X$ .

The reaction rate (e.g.,  $v_0$  or  $v_{\max}$ ) is typically expressed in moles of product formed per unit of time (or moles of substrate consumed per unit of time). The raw calorimetric signal is expressed as a power (e.g.,  $\mu\text{cal}/\text{sec}$  or  $\mu\text{J}/\text{sec}$ ). This heat rate is simply equal to the reaction rate multiplied by the enthalpy change for the reaction as shown in Eq. (23).

$$\frac{\delta Q}{\delta t} = \frac{\delta n}{\delta t} \times \Delta H \quad (23)$$

The raw calorimetric signal is thus a direct measure of the reaction rate making the calorimeter an ideal instrument for kinetic studies. The enthalpy changes for most enzyme-catalyzed reactions range from  $-10$  to  $-100$  kcal/mol, allowing reaction rates from 10 to 100 pmol/sec to be accurately measured.

Kinetic data for an enzyme-catalyzed reaction described by the Michaelis-Menton rate equation are simulated in Fig. 12.

In these simulations, the total enzyme concentration,  $[E]_t$ , is  $5 \times 10^{-6}$  M. Substrate was added to produce the variable concentrations as listed on the  $x$ -axis. The dependence of the reaction rate on  $K_m$  or  $k_{\text{cat}}$  is illustrated by holding one variable constant (either  $K_m$  or  $k_{\text{cat}}$ ) and plotting the rate curves for four different values of the other variable. In Fig. 12A, the  $k_{\text{cat}}$  value is  $80 \text{ sec}^{-1}$  for all of the rate curves shown and the values of  $K_m$  appear on the plot. In Fig. 12B, the  $K_m$  value is  $0.075 \text{ M}^{-1}$  for all of the rate curves shown and the values of  $k_{\text{cat}}$  used for the four simulations are shown on the plot. It should be obvious that calorimetric

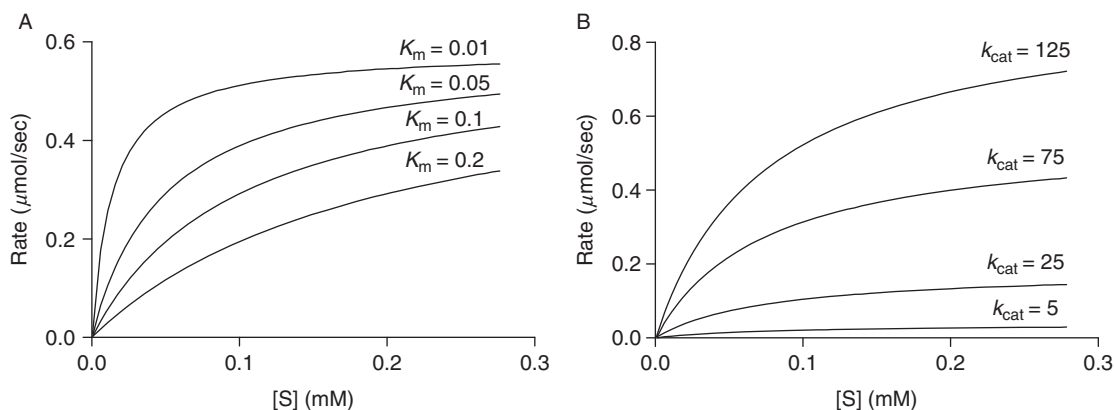


**Fig. 12** Representation of the effect of  $K_m$  and  $k_{\text{cat}}$  on the hyperbolic curve shape of kinetic ITC data. The data in panel A vary with respect to  $K_m$  with a constant  $k_{\text{cat}}$  value of  $80 \text{ sec}^{-1}$ . The data in panel B vary with respect to  $k_{\text{cat}}$  with a constant  $K_m$  value of  $0.075 \text{ M}^{-1}$ . The data in both panels were simulated for an  $[E]_t = 5 \mu\text{M}$ .

data (the rate curve) could easily be curve fit to yield the appropriate values for both the nonlinear parameters  $K_m$  and  $k_{cat}$  and the linear parameters  $[E]_t$  and  $\Delta H$ . The value given for  $[E]_t$  illustrates the sensitivity of the ITC technique and is typical for these types of experiments. The  $\Delta H$  value is not listed as its influence on the raw data is linear and the only concern here is that the heat rate would be detectable in the ITC.

## B. Planning the Experiment

As with the ITC-binding experiments described previously, there are several steps to running an ITC kinetic experiment. These steps are (i) planning the experiment, (ii) preparing the substrate and enzyme solutions, (iii) collecting the raw ITC kinetic data, (iv) collecting the blank (substrate and protein dilutions), (v) correcting the raw ITC data, and (vi) analysis of the corrected titration data to provide estimates of the kinetic parameter values.

There are two different ITC methods for performing an enzyme kinetic experiment: [single injection (DIE) and multiple injections (or continuous)]. The first step in planning either ITC kinetic experiment is to determine optimal concentrations for the enzyme and substrate solutions. ITC kinetic experiments require a concentration of substrate large enough to produce an accurately measurable heat rate ( $>10 \mu\text{cal}/\text{sec}$  for single injection experiments and  $>2 \mu\text{cal}/\text{sec}$  for the initial injections in a multiple injection experiment). The initial heat rate produced per injection can be calculated using Eq. (23) and estimates the reaction rate and the  $\Delta H$ .

When performing a single injection ITC kinetic experiment, the substrate solution is injected into the cell containing the enzyme solution producing a heat response which eventually returns to baseline after all of the substrate has reacted. A second injection of substrate can be made to collect additional information about the reaction (e.g., the presence or absence of product inhibition). Simulated data for a single injection experiment are shown in Fig. 13.

The thermogram shown is for an experiment in which the enzyme concentration in the ITC cell is  $5 \mu\text{M}$ ,  $\Delta H = -50 \text{ kcal}/\text{mol}$ ,  $K_m = 0.075 \text{ M}^{-1}$ , and  $k_{cat} = 80 \text{ sec}^{-1}$ . The substrate solution concentration was  $1 \text{ mM}$  and the injected volume was  $40 \mu\text{l}$ . The substrate was completely consumed after about  $1500 \text{ sec}$ . The analysis of these data will be described in a later section. Figure 14 shows simulated data for four different experiments in which all of the parameters except  $\Delta H$  are the same as those for the data shown in Fig. 13.

Satisfactory data are obtained in the three simulations with the larger  $\Delta H$  values. In the case of the experiment with the lowest  $\Delta H$  value ( $-5 \text{ kcal}/\text{mol}$ ), the enzyme concentration or the amount of substrate would need to be increased to yield an analyzable data set with an adequate initial heat rate ( $>10 \mu\text{cal}/\text{sec}$ ).

The continuous method of ITC kinetic experimentation makes use of multiple titrations that are spaced such that subsequent titrant additions are performed when the heat rate has reached a steady state. It is important that each subsequent

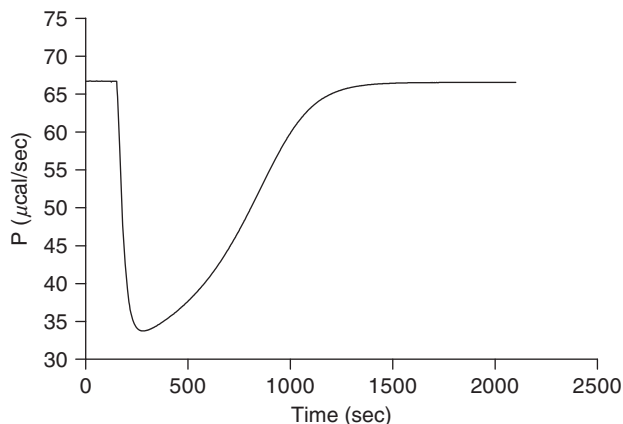


**Fig. 13** Simulation of a single injection kinetic ITC experiment. This simulation was for the following parameters:  $k_{\text{cat}} = 80 \text{ sec}^{-1}$ ,  $K_m = 0.075 \text{ M}^{-1}$ ,  $\Delta H = -50 \text{ kcal/mol}$ , and  $[E]_t = 4.5 \text{ } \mu\text{M}$ .

addition of substrate is made prior to significant reaction of the substrate. The difference in the signal plateau between each injection is used to determine the reaction rate at that step. This information is used to create a plot of the reaction rate (in units of power) versus total substrate concentration. This plot can then be fit to determine the kinetic parameters for the reaction. The analysis of the data obtained with the continuous method assumes that there is no significant substrate degradation during the time between injections. The main advantage of the

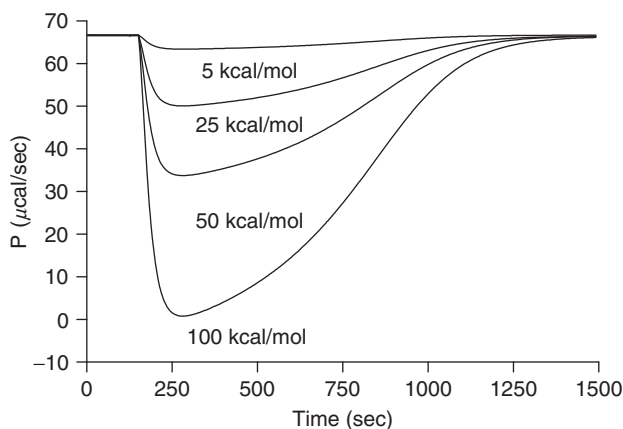


**Fig. 14** Representation of the effect of  $\Delta H$  on the size of single injection curves. All of these curves have the following parameters:  $k_{\text{cat}} = 80 \text{ sec}^{-1}$ ,  $K_m = 0.075 \text{ M}^{-1}$ , and  $[E]_t = 4.5 \text{ } \mu\text{M}$ . The  $\Delta H$  values vary from 5 to 100 kcal/mol.

continuous method over the single injection method is higher accuracy in determining kinetic parameters. The only disadvantage is that it is unable to determine  $\Delta H_{\text{app}}$  because the titration points do not allow for the complete reaction of the substrate prior to adding more substrate. This can be overcome by performing a single injection experiment to determine the  $\Delta H_{\text{app}}$ .

Simulated data for a multiple injection experiment are shown in Fig. 15.

The thermogram shown is for an experiment in which the enzyme concentration in the ITC cell is  $5 \mu\text{M}$ ,  $\Delta H = -50 \text{ kcal/mol}$ ,  $K_m = 0.075 \text{ M}^{-1}$ , and  $k_{\text{cat}} = 80 \text{ sec}^{-1}$ . The substrate solution concentration was  $1 \text{ mM}$  and there were  $30 \times 3 \mu\text{l}$  injections performed at 100-sec intervals. The analysis of these data will be described in a later section. Figure 16 shows simulated data for four different experiments in which all of the parameters except  $\Delta H$  are the same as those for the data shown in Fig. 15.

Satisfactory data are obtained in the two simulations with the larger  $\Delta H$  values. In the case of the experiments with the two lowest  $\Delta H$  values ( $-5$  and  $-25 \text{ kcal/mol}$ ), the enzyme concentration or the amount of substrate would need to be increased to yield an analyzable data set with an adequate initial heat rate ( $>2 \mu\text{cal/sec}$ ).

## C. Running the Kinetic ITC Experiment

### 1. Solution Preparation and Handling

Once the necessary concentrations have been estimated, the next step is to prepare the ligand and macromolecule solutions. The solution preparation techniques for both single injection and continuous kinetic experiments are identical. As we discussed in the section on ITC-binding experiments, it is imperative that

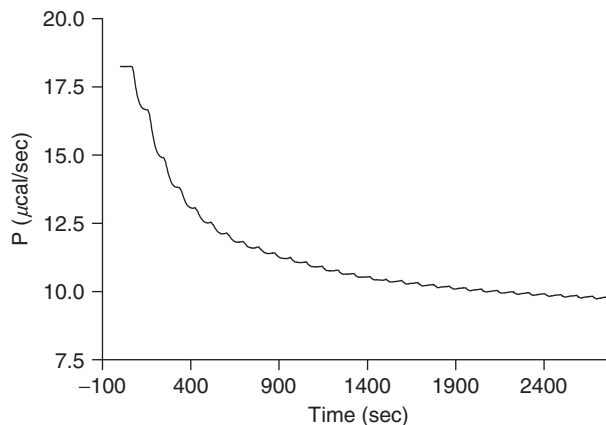


**Fig. 15** Simulation of a multiple injection kinetic ITC experiment. This simulation was for the following parameters:  $k_{\text{cat}} = 80 \text{ sec}^{-1}$ ,  $K_m = 0.075 \text{ M}^{-1}$ ,  $\Delta H = -50 \text{ kcal/mol}$ , and  $[E]_t = 4.5 \mu\text{M}$ .

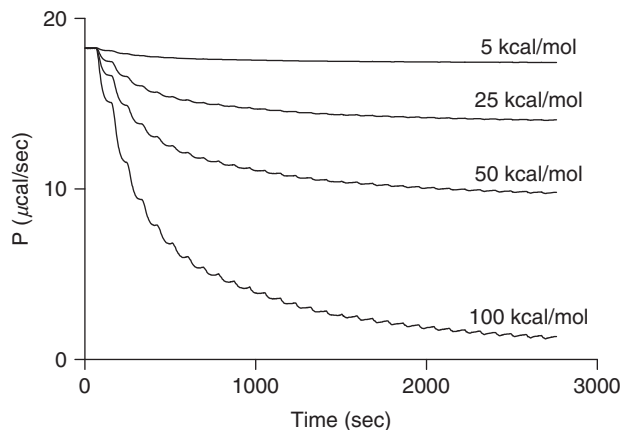


**Fig. 16** Representation of the effect of  $\Delta H$  on the size of multiple injection titration curves. All of these curves have the following parameters:  $k_{\text{cat}} = 80 \text{ sec}^{-1}$ ,  $K_m = 0.075 \text{ M}^{-1}$ , and  $[E]_t = 4.5 \text{ } \mu\text{M}$ . The  $\Delta H$  values vary from 5 to 100 kcal/mol.

accurate concentrations are known for both the substrate and the enzyme. Concentration errors in either  $[S]$  or  $[E]_t$  will result in incorrect values for  $\Delta H_{\text{app}}$ ,  $K_m$ , and  $k_{\text{cat}}$ . These solutions should be prepared as accurately as possible, and whenever possible the concentrations should be verified using an analytical procedure (e.g., UV-VIS absorbance). In addition to extremely accurate knowledge of the concentrations of both the substrate and the protein, it is also essential that these two solutions are identical with respect to buffer composition (salt, pH, and so on). The best solution to this problem is to exhaustively dialyze the macromolecule (e.g., dialyzing 1 ml of concentrated protein solution in two 1-liter changes of buffer over the course of 48 h) and prepare the substrate solution in the resulting dialysate (in the dialysis example above some of the second liter of buffer would be saved to prepare substrate solutions). As discussed previously with the ITC-binding experiments, both the protein and substrate solutions should be degassed prior to filling the cell and the injection syringe. This serves to minimize the generation of bubbles and an accompanying erroneous heat signal.

## 2. Collecting Raw ITC Data

The collection of raw data for ITC kinetic experiments is similar to the experimental protocol for binding experiments. The main difference is the spacing between injections. If performing a single injection experiment, the instrument is programmed to perform one injection. If two injections are desired (to investigate product inhibition for example), then the spacing between injections should be quite large (e.g., 30 min) to allow ample time for the baseline to return to its starting point. If the multiple injection method of kinetic analysis is used, the

instrument should be programmed to perform as many injections as needed, and the spacing between injections should be set such that the signal has achieved a steady state maximum heat rate when the next injection takes place. This will likely require the experimenter to watch the titration closely and tailor the spacing in between injections to the specific reaction and concentrations being studied (an injection interval of 100 sec was used in producing the data set shown in Fig. 15).

### 3. Correcting the Raw ITC Data

As discussed with ITC-binding experiments, performing exhaustive dialysis of the protein and then preparing the substrate solution with the resulting dialysate will reduce heats of dilution significantly. However, it is still important to correct for the heats of dilution of the substrate and enzyme solutions. The first blank experiment is performed by injection of the substrate solution into buffer. It is important that the volume injected here is the same as the injection volume(s) used in the kinetic experiment. To perform the blank experiment for the dilution of the enzyme, buffer is injected into the protein solution at the same concentration used in the kinetic experiment. A rigorous approach would also include a third blank experiment where buffer is injected into buffer. All of these blank heat effects would be subtracted to yield the corrected heat (heat rate) of reaction.

### D. Analyzing the Kinetic ITC Data

The ITC kinetic data are analyzed using nonlinear regression analysis techniques. Commercial calorimeters come with the software (programs) that is required for the analysis of ITC kinetic raw data. The analysis is transparent to the user who only needs to determine which type of experiment to perform (single injection, multiple injection, substrate only, substrate + inhibitor, etc.) and to select the appropriate analysis routine. The linear parameters are  $[E]_t$  and  $\Delta H$ , and the nonlinear parameters are  $K_m$  and  $k_{cat}$ .

The analysis of single injection data (like that shown in Fig. 15) is based on first estimating the molar enthalpy change for the conversion of substrate to product. The value of the enthalpy change,  $\Delta H$ , is determined by integration of the thermogram and Eq. (24).

$$\Delta H = \frac{\int_{t=0}^{\infty} \frac{dQ}{dt} dt}{[S]_{t=0} V_{cell}} \quad (24)$$

This equation describes the molar enthalpy change for the reaction,  $S \rightarrow P$ , where  $\partial Q/\partial t$  is the excess power or reaction heat rate,  $[S]_{t=0}$  is the concentration of ligand at time zero, and  $V_{cell}$  is the volume of the calorimeter cell. The initial

velocity ( $V_0$ ) can be estimated immediately after an injection of substrate. The maximal velocity,  $V_{\max}$ , can be estimated immediately after an injection of enough substrate to saturate the enzyme.  $K_m$  can be estimated from ITC-binding data under conditions where the substrate binds but is not converted to product (titrations done in the presence of a noncompetitive inhibitor or in the absence of a required reactant, cofactor, or coenzyme). The initial rate, obtained under substrate saturating conditions, can be used with the total macromolecule concentration to estimate  $k_{\text{cat}}$  and  $K_m$  for a system that follows Michaelis-Menton kinetics (see Eq. 22). Figure 17 shows a fit of the data in Fig. 13, first converted to reaction rate as a function of  $[S]$  and then fit to a Michaelis-Menton model.

In this case, the points shown represent data taken at equal intervals from the continuous curve of the thermogram from a single injection of substrate. The best-fit parameter values returned from the nonlinear regression ( $K_m = 0.077 \text{ M}^{-1}$  and  $k_{\text{cat}} = 89 \text{ sec}^{-1}$ ) are very close to the parameters that were used to generate the simulated data set ( $K_m = 0.075 \text{ M}^{-1}$  and  $k_{\text{cat}} = 80 \text{ sec}^{-1}$ ).

The analysis methods for continuous ITC kinetic experiments are slightly different than those used for single injection kinetic experiments. As mentioned previously,  $\Delta H$  cannot be determined from a continuous experiment since the continuous method does not allow for the complete reaction of substrate prior to starting subsequent injections. If the  $\Delta H$  value has been determined from a single injection experiment,  $V_0$  can be calculated using the same equation used for the single injection experiment. The advantage of the continuous experiment is that it produces discrete values of  $V_0$  as a function of total substrate concentration for well-determined values of the substrate concentration (i.e., the total substrate concentration added to the solution is used instead of a single concentration of substrate at time zero  $[S]_{t=0}$ ). This allows iteration on the rate equation with fixed

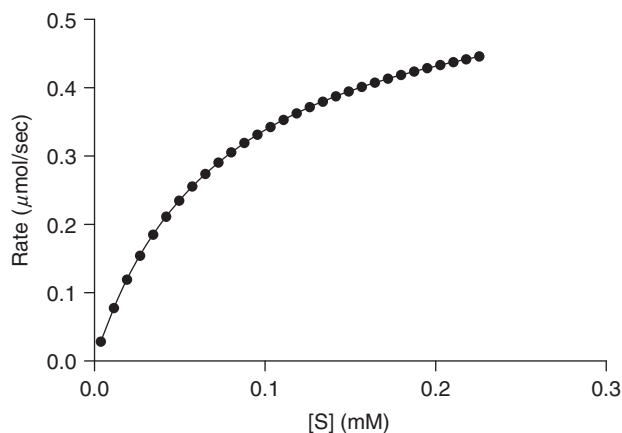


**Fig. 17** Representative fit of the simulated single injection data shown in Fig. 13. The data were fit with nonlinear regression analysis resulting in “best-fit” parameters of  $k_{\text{cat}} = 88.6 \text{ sec}^{-1}$  and  $K_m = 0.077 \text{ M}^{-1}$ .

values for the substrate concentration leading to less statistical error in the best-fit parameters for  $k_{\text{cat}}$  and  $K_m$ . Figure 18 shows a fit of the data in Fig. 15, first converted to reaction rate as a function of [S] and then fit to a Michaelis-Menton model.

In this case, the points shown are for each of the 30 substrate injections. The best-fit parameter values returned from the nonlinear regression ( $K_m = 0.072 \text{ M}^{-1}$  and  $k_{\text{cat}} = 85 \text{ sec}^{-1}$ ) are again very close to the parameters that were used to generate the simulated data set ( $K_m = 0.075 \text{ M}^{-1}$  and  $k_{\text{cat}} = 80 \text{ sec}^{-1}$ ).

### E. Models

The only model that is implemented in currently available software is for systems that follow simple Michaelis–Menton kinetics (see Eq. 22). The canned programs assume, for example, that there is no product inhibition. In principle, an advanced user could write more complicated rate expressions and use a program like Mathematica 5.0™ to perform the nonlinear regression (curve fit) of the experimental thermogram to the more complex model. The calorimetric data are independent of the model and a direct measure of the reaction rate as a function of time, [S], [E]<sub>t</sub>, and any competing reactions, for example, the influence of regulatory or inhibitory compounds.

### F. Summary

ITC kinetic experiments take advantage of the fact that a calorimeter is a universal detector (almost all chemical reactions are accompanied by a change in heat). The recent literature has demonstrated the use of ITC in characterizing a number of enzymes by determining kinetic (as well as thermodynamic) constants. ITC experiments can be done on solutions that are either homogeneous or

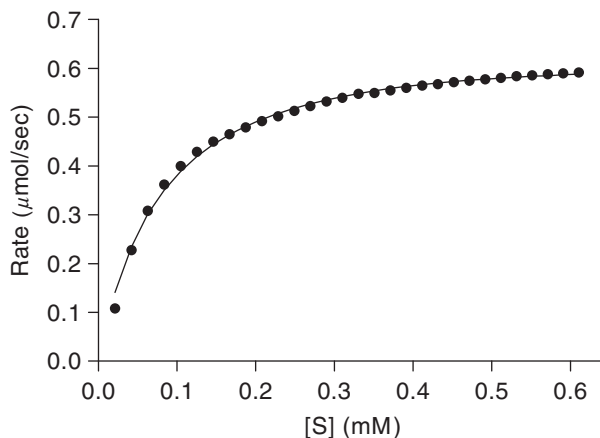


**Fig. 18** Representative fit of the simulated multiple injection data shown in Fig. 15. The data were fit with nonlinear regression analysis resulting in “best-fit” parameters of  $k_{\text{cat}} = 71.3 \text{ sec}^{-1}$  and  $K_m = 0.085 \text{ M}^{-1}$ .

heterogeneous (e.g., cell suspensions), or are turbid or opaque. ITC is also sensitive enough (noise levels  $>0.01 \mu\text{cal/sec}$ ) that enzyme concentrations and volumes required are similar to those needed for spectrophotometric analyses. There currently exists a database of ITC enzyme studies that can be used to design experiments on as yet unstudied enzymes with minimal method development. The ITC technique generates a complete reaction rate curve in a single experiment and the values of  $[\text{E}]_t$ ,  $\Delta H$ ,  $K_m$ , and  $k_{\text{cat}}$  have been shown to be in good agreement with the values for these parameters determined by other techniques.

The conclusions that can be drawn for the above discussions of the ITC kinetic experiment, the nonlinear fitting of the ITC data, and data interpretation are listed below.

- It is important in planning the ITC kinetic experiment that reasonable concentrations be chosen for the enzyme and the substrate. This may require a guess at the  $K_m$ ,  $k_{\text{cat}}$ , and  $\Delta H$  values and/or one or more scoping experiments in which a substrate is injected into an the enzyme solution to determine the approximate initial heat rate and total heat of reaction.
- In a single injection experiment, there must be enough enzymes in the calorimeter cell to convert all of the substrate to product in a reasonable time (e.g., 30–60 min).
- Enzyme concentrations in the calorimeter cell in the range of 1 nM to 10  $\mu\text{M}$  are typical for these experiments.
- The substrate concentration (in the injection syringe) should be  $10^3$ – $10^4$  more concentrated than the enzyme, larger than the  $K_m$ , and in excess of the enzyme.
- In single injection experiments, the injected volume should be in the range of 25–50  $\mu\text{l}$ . In the continuous experiments, the injection volumes should be in the range of 2–5  $\mu\text{l}$  for each injection of the substrate solution.
- It is possible to perform a kinetic experiment by injection of the enzyme into a limited amount of substrate in the calorimeter cell.
- The values for  $K_m$  and  $k_{\text{cat}}$  can be determined with reasonable accuracy in less than 1 h in a single experiment
- The linear parameters  $[\text{E}]_t$  and  $\Delta H$  will be better determined than the nonlinear parameters  $K_m$  and  $k_{\text{cat}}$ .

The only limitation of the ITC technique at present is that modeling is limited to systems obeying simple Michaelis–Menton kinetics. This is actually a limitation of the currently available software in that the ITC will generate a complete reaction rate curve for any system that produces a measurable heat.

---

---

---

## V. Conclusions

Fundamental areas of biology, molecular biology, biochemistry, and biophysics are dedicated to determining the relationships between the structure and function of proteins and nucleic acids.

Biologists need to better understand the recognition of small molecules for specific interaction sites on larger molecules and the nature of the weak individual interactions that can result in very high affinity. Ray Salemme, chief scientific officer of 3-D Pharmaceuticals, was quoted in a *C&E News* feature article as saying, “The initial expectation of structure-based drug design, that you were going to be able to design molecules and they were going to work right out of the box, was unrealistic. We didn’t understand the thermodynamics well enough” (Henry, 2001). The use of ITC methods to probe the energetics of biologically relevant binding interactions is somewhat underappreciated (Chaires, 2006; Freyer *et al.*, 2007c). ITC provides a universal approach to determining the molecular nature of noncovalent interactions involved in the binding of small molecules to biopolymers (and even biopolymers to other biopolymers). In particular, ITC-binding experiments can yield a complete set of thermodynamic parameters for complex formation in a single experiment (Christensen *et al.*, 1966; Doyle, 1997; Eatough *et al.*, 1985; Wiseman *et al.*, 1989). The parsing of the Gibbs Free Energy change into the enthalpy and entropy contributions can provide new insight into the molecular nature of the binding interaction being studied (Freyer *et al.*, 2007b; Ladbury, 1996), also see the Chapter 1 by Garbett and Chaires, this volume. The energetic information is fundamental to not only understanding naturally occurring binding interactions but is particularly useful in drug discovery studies (Freyer *et al.*, 2007a,c; Ladbury, 2001, 2004).

Biologists also need to better understand the catalytic activity of enzymes and the affinity of a substrate for a specific active site. The kinetic behavior of enzymes (an obvious biopolymer function of interest) is important to not only understanding biochemical pathways and catalytic mechanisms but is again a fruitful area for drug discovery and development. The use of ITC methods to probe the kinetics of enzymes is a rather recent development (Todd and Gomez, 2001) and actually a rediscovery of some earlier work (Morin and Freire, 1991; Spink and Wadso, 1976; Watt, 1990; Williams and Toone, 1993). Again, ITC provides a universal approach to determining the kinetic behavior of enzymes and can yield in a single experiment a complete set of kinetic parameters for an enzyme-catalyzed reaction.

Hopefully, the information provided in this chapter will encourage researchers to further explore the advantages of the ITC methods for their studies of biopolymer interactions.

## Acknowledgments

We would like to thank Jonathan (Brad) Chaires, Jack Correia, Joel Tellinghuisen, Jim Thomson, and W. David Wilson for their contributions to this chapter and encouragement. Supported by an NAU Prop 301 award and ABRC grants 0014 and 0015.

## References

- Ababou, A., and Ladbury, J. E. (2006). Survey of the year 2004: Literature on applications of isothermal titration calorimetry. *J. Mol. Recognit.* **19**, 79–89.

- Bandman, U., Monti, M., and Wadso, I. (1975). Microcalorimetric measurements of heat production in whole blood and blood cells of normal persons. *Scand. J. Clin. Lab. Invest.* **35**, 121–127.
- Beaudette, N. V., and Langerman, N. (1978). An improved method for obtaining thermal titration curves using micromolar quantities of protein. *Anal. Biochem.* **90**, 693–704.
- Biltonen, R. L., and Langerman, N. (1979). Microcalorimetry for biological chemistry: Experimental design, data analysis, and interpretation. *Methods Enzymol.* **61**, 287–318.
- Black, J. (1803). “Lectures on the Elements of Chemistry.” Mundell & Son, Edinburgh.
- Bundle, D. R., and Sigurskjold, B. W. (1994). Determination of accurate thermodynamics of binding by titration microcalorimetry. *Methods Enzymol.* **247**, 288–305.
- Chaires, J. B. (2006). A thermodynamic signature for drug-DNA binding mode. *Arch. Biochem. Biophys.* **453**, 26–31.
- Christensen, J., Hansen, L. D., and Izatt, R. M. (1976). “Handbook of Proton Ionization Heats and Related Thermodynamic Quantities.” John Wiley & Sons, Inc, New York, NY.
- Christensen, J. J., Izatt, R. M., and Eatough, D. (1965). Thermodynamics of metal cyanide coordination. V. Log  $K$ ,  $\Delta H^\circ$ , and  $\Delta S^\circ$  values for the  $Hg_2 + -cn$ -system. *Inorg. Chem.* **4**, 1278–1280.
- Christensen, J. J., Izatt, R. M., Hansen, L. D., and Partridge, J. M. (1966). Entropy titration. A calorimetric method for the determination of  $\Delta G$ ,  $\Delta H$  and  $\Delta S$  from a single thermometric titration. *J. Phys. Chem.* **70**, 2003–2010.
- Christensen, J. J., Wrathall, D. P., Oscarson, J. L., and Izatt, R. M. (1968). Theoretical evaluation of entropy titration method for calorimetric determination of equilibrium constants in aqueous solution. *Anal. Chem.* **40**, 1713–1717.
- Cliff, M. J., Gutierrez, A., and Ladbury, J. E. (2004). A survey of the year 2003 literature on applications of isothermal titration calorimetry. *J. Mol. Recognit.* **17**, 513–523.
- Correia, J. J., and Chaires, J. B. (1994). Analysis of Drug-DNA binding Isotherms: A Monte Carlo approach. In “Numerical Computation Methods Part B, Methods in Enzymology” (L. Brand, and M. L. Johnson, eds.), Vol. 240, pp. 593–614. Academic Press, San Diego, CA.
- Doyle, M. L. (1997). Characterization of binding interactions by isothermal titration calorimetry. *Curr. Opin. Biotechnol.* **8**, 31–35.
- Eatough, D. (1970). Calorimetric determination of equilibrium constants for very stable metal-ligand complexes. *Anal. Chem.* **42**, 635–639.
- Eatough, D. J., Lewis, E. A., and Hansen, L. D. (1985). Determination of  $\Delta H$  and  $K_{eq}$  values. In “Analytical Solution Calorimetry” (K. Grime, ed.), pp. 137–161. John Wiley & Sons, New York, NY.
- Fasman, G. D. (1976). “Handbook of Biochemistry: Section D Physical Chemical Data.” CRC Press, Boca Raton, FL.
- Fisher, H. F., and Singh, N. (1995). Calorimetric methods for interpreting proteinligand interactions. *Methods Enzymol.* **259**, 194–221.
- Freiere, E. (2004). Isothermal titration calorimetry: Controlling binding forces in lead optimization. *Drug Discov. Today* **1**, 295–299.
- Freire, E., Mayorga, O. L., and Straume, M. (1990). Isothermal titration calorimetry. *Anal. Chem.* **62**, 950A–959A.
- Freyer, M. W., Buscaglia, R., Cashman, D., Hyslop, S., Wilson, W. D., Chaires, J. B., and Lewis, E. A. (2007a). Binding of Netropsin to several DNA constructs: Evidence for at least two different 1:1 complexes formed from an -A2T2- containing ds-DNA construct and a single minor groove binding ligand. *Biophys. Chem.* **126**, 186–196.
- Freyer, M. W., Buscaglia, R., Hollingsworth, A., Ramos, J. P., Blynn, M., Pratt, R., Wilson, W. D., and Lewis, E. A. (2007b). Break in the heat capacity change at 303 K for complex binding of netropsin to AATT containing hairpin DNA constructs. *Biophys. J.* **92**(7), 2516–2522.
- Freyer, M. W., Buscaglia, R., Kaplan, K., Cashman, D., Hurley, L. H., and Lewis, E. A. (2007c). Biophysical studies of the c-MYC NHE III<sub>1</sub> promoter: Model quadruplex interactions with a cationic porphyrin. *Biophys. J.* **92**, 2007–2015.

- Freyer, M. W., Buscaglia, R., Nguyen, B., Wilson, W. D., and Lewis, E. A. (2006). Binding of netropsin and DAPI to an A2T2 DNA hairpin: A comparison of biophysical techniques. *Anal. Biochem.* **355**, 259–266.
- Hansen, L. D., Christensen, J. J., and Izatt, R. M. (1965). Entropy titration. A calorimetric method for the determination of  $\Delta G^\circ$  (k),  $\Delta H^\circ$  and  $\Delta S^\circ$ . *J. Chem. Soc. Chem. Commun.* **3**, 36–38.
- Hansen, L. D., Lewis, E. A., and Eatough, D. J. (1985). Instrumentation and data reduction. In “Analytical Solution Calorimetry” (K. Grime, ed.), pp. 57–95. John Wiley & Sons, New York, NY.
- Henry, C. M. (2001). Structure-based drug design. *C&E News* **79**, 69–74.
- Indyk, L., and Fisher, H. F. (1998). Theoretical aspects of isothermal titration calorimetry. *Methods Enzymol.* **295**, 350–364.
- Ladbury, J. (2004). Application of isothermal titration calorimetry in the biological sciences: Things are heating up!. *Biotechniques* **37**, 885–887.
- Ladbury, J. E. (1996). Just add water! The effect of water on the specificity of protein–ligand binding sites and its potential application to drug design. *Chem. Biol.* **3**, 973–980.
- Ladbury, J. E. (2001). Isothermal titration calorimetry: Application to structure-based drug design. *Thermochim. Acta* **380**, 209–215.
- Langerman, N., and Biltonen, R. L. (1979). Microcalorimeters for biological chemistry: Applications, instrumentation and experimental design. *Methods Enzymol.* **61**, 261–286.
- Lavoisier, A. L., and Laplace, P. S. (1780). Memoire sur la Chaleur. *Mem. Acad. Roy. Sci.* 355–408.
- Lewis, E. A., and Murphy, K. P. (2005). Isothermal titration calorimetry. *Methods Mol. Biol.* **305**, 1–16.
- Monti, M., Brandt, L., Ikomi-Kumm, J., and Olsson, H. (1986). Microcalorimetric investigation of cell metabolism in tumour cells from patients with non-Hodgkin lymphoma (NHL). *Scand. J. Haematol.* **36**, 353–357.
- Morin, P. E., and Freire, E. (1991). Direct calorimetric analysis of the enzymatic activity of yeast cytochrome c oxidase. *Biochemistry* **30**, 8494–8500.
- Spink, C., and Wadso, I. (1976). Calorimetry as an analytical tool in biochemistry and biology. *Methods Biochem. Anal.* **23**, 1–159.
- Todd, M. J., and Gomez, J. (2001). Enzyme kinetics determined using calorimetry: A general assay for enzyme activity? *Anal. Biochem.* **296**, 179–187.
- Watt, G. D. (1990). A microcalorimetric procedure for evaluating the kinetic parameters of enzyme-catalyzed reactions: Kinetic measurements of the nitrogenase system. *Anal. Biochem.* **187**, 141–146.
- Williams, B. A., and Toone, E. J. (1993). Calorimetric evaluation enzyme kinetics parameters. *J. Org. Chem.* **58**, 3507–3510.
- Wiseman, T., Williston, S., Brandts, J. F., and Lin, L. N. (1989). Rapid measurement of binding constants and heats of binding using a new titration calorimeter. *Anal. Biochem.* **179**, 131–137.